INVITED REVIEW

Limiters and wall treatments in applied turbulence modeling

P A Durbin

Department of Aerospace Engineering, Iowa State University, 2271 Howe Hall, Ames, IA 50011, USA

E-mail: durbin@iastate.edu

Abstract

Issues in practical use of turbulence models include large strain limiters, wall functions and roughness corrections. Motivations for studying these topics are provided and various recent developments in modeling are reviewed. Inequalities and consistency between wall and outer region models are discussed. New elliptic relaxation models are also surveyed. These include elliptic blending and changes of the dependent variable in scalar eddy viscosity models.

1. Introduction

Turbulence models existed prior to the advent of digital electronic computers. With the availability of increasingly powerful computers, they have come into their own as powerful tools for practical engineering analysis. To meet the needs of complex geometries, early algebraic formulae have given way to transport equations and constitutive formulae. Constraints of coordinate independence, Galilean invariance and geometry independence have guided their development. These are fundamental requirements, applicable to any model.

As much as one might prefer to limit constraints on model formulations to such fundamental principles, the demands of accurate prediction have required researchers to propose additional conditions. These may be based on empirical evidence or on mathematical inequalities. Often they are implemented as bounds on variables. Section 2 of this paper reviews some of the ideas on *constraints for practical turbulence modeling*. The bounds that have been devised prevent spurious production of turbulent kinetic energy and impose realizability constraints. These two turn out to be closely related.

The second topic of this review is the *wall function*. Analysis of flow in complex geometries can impose severe demands on mesh resolution. Wall functions are a firmly established method to reduce the demands on meshing. The idea of a wall function dates

back to the early days of turbulence modeling. Recent developments have been directed to making them more flexible. Although they are primarily a pragmatic device, wall functions have a solid theoretical foundation in turbulence theory. They stem from notions about universality of the *law of the wall*. As such, they are based on a high Reynolds number assumption. At finite Reynolds number, the conditions for universality can be violated by pressure gradients, surface curvature or other departures from the ideal. Various revisions to wall function methodology have attempted to accommodate such effects. Even within the scope of the formal theory, the classical wall function is further limited to large y_+. A good deal of recent work has been on permitting the grid to begin at low y_+.

However, a more pragmatic difficulty is the tendency for wall function computations to be grid-dependent. In asymptotic theory, the law of the wall is an inner region which matches to an outer region within an overlap layer. The wall function provides a representation of the inner region and the turbulence model represents the outer region. In classical wall functions, the transition between these two representations is assumed to occur in the overlap layer— that is, in the logarithmic layer. However, any pre-set grid might produce a transition point that does not lie in the overlap layer—if such a layer even exists. Then the two representations are being *patched* rather than *matched*: the solution depends on the patching point because it does not occur in a region that is common to the inner and outer solutions. By making the wall function consistent with the outer model throughout the wall layer, sensitivity to the patching point can be reduced. The holy grail is a grid-independent formulation.

As an operational matter, that goal can be elusive. The wall function is meant to permit a relatively coarse near-wall grid. Even if the formulation is consistent, grid dependence may be inevitable. Grid dependence is caused by coarseness of the grid. In principle, one might place a fine grid just above the top of the wall function layer. While this approach can be used to prove the consistency of how the two layers are patched (Kalitzin *et al* 2005), that is not how wall functions are used in practice. For example, in a standard finite-volume mesh, if the first cell center is at $y_+ = 20$, the second is at $y_+ = 60$. Even if the wall function provides an accurate match to the model, the computation will be grid-dependent owing to the coarse mesh.

The final section of the present paper describes some developments of the *elliptic relaxation method*. Elliptic relaxation is a method to introduce non-local wall effects on the turbulence field near a boundary. Consistent with the theme of modeling for complex geometries, the objective is to solve an elliptic equation that will produce the wall effect through the application of boundary conditions. The turbulence scale controls the extent of interaction.

This paper admittedly is limited in its perspective. It is not meant to cite the many developments that have occurred in Reynolds averaged modeling during recent years, but simply to cite a few that have been of concern to the present author.

2. Inequalities to avoid anomalies

Constraints on model coefficients have become an indispensable component of closure modeling. They may derive either from empirical evidence or from mathematical conditions. A notable example of the former is the shear stress limit devised by Menter (1992). He noted that the stress-intensity ratio predicted by two-equation models scales with the ratio of production to dissipation as

$$\frac{-\overline{uv}}{k} = \sqrt{\frac{\mathcal{P}}{\varepsilon}}\sqrt{C_\mu}. \tag{1}$$

Two-equation models evaluate an eddy viscosity from predictions of k and of the correlation timescale T:

$$\nu_T = C_\mu k T, \tag{2}$$

where C_μ is a coefficient of proportionality. Equation (1) derives from the formula for production in parallel shear flow, $\mathcal{P} = -\overline{uv}\partial_y U$, with the eddy viscosity model $-\overline{uv} = \nu_T \partial_y U$, after substituting the eddy viscosity formula (2) with $T = k/\varepsilon$.

Experiments show that the stress-intensity ratio is about 0.3 in shear layers. While there is variation about this value, the stress-intensity ratio certainly does not grow with $\mathcal{P}/\varepsilon$ in the manner of equation (1). If it is required that $-\overline{uv}/k \leqslant 0.3$, then the eddy viscosity is constrained by

$$\nu_T \leqslant \frac{0.3k}{|\partial_y U|}.$$

Denoting the rate of strain tensor by $S_{ij} = \frac{1}{2}(\partial_j U_i + \partial_i U_j)$ and its magnitude by $|\boldsymbol{S}|^2 = S_{ij}S_{ji}$, this constraint can be generalized to

$$\nu_T \leqslant \frac{0.3k}{\sqrt{2}|\boldsymbol{S}|}, \tag{3}$$

because $\partial_y U^2 = 2|\boldsymbol{S}|^2$. Menter devised his SST modification of the k–ω model from this starting point. It serves as an informative example of an empirically based constraint. The constraint was implemented as the limiter

$$\nu_T = \min\left[\frac{k}{\omega}, \frac{0.3k}{\sqrt{2}|\boldsymbol{S}|F_2(y)}\right],$$

where F_2 is a blending function that tends to zero outside the boundary layer (Menter used the vorticity $|\boldsymbol{\omega}|$ instead of the rate of strain $|\boldsymbol{S}|$ in his SST model).

A constraint that derives wholly from mathematical considerations has received a good deal of attention recently. The most common, general purpose, scalar eddy viscosity models, k–ε and k–ω, are subject to a spurious overproduction of turbulent kinetic energy in highly strained flows. Although this goes by the name 'stagnation point anomaly', it arises generally under high rates of strain and can be seen in turbine and compressor passages. It is manifested by turbulent intensities growing to highly unphysical levels. Anomalous turbulent kinetic energy levels are illustrated by the panel at the right of figure 1. When is the rate of strain 'high'? An objective definition is: when the rate of strain is large enough for the model to violate a physical bound on energy production.

The full formula for production is

$$\mathcal{P} = -\overline{u_i u_j} S_{ij}. \tag{4}$$

In principal axes of the rate of strain tensor is

$$\mathcal{P} = -\overline{u_1 u_1} S_{11} - \overline{u_2 u_2} S_{22} - \overline{u_3 u_3} S_{33}.$$

In incompressible flow, $S_{ii} = 0$, so at least one $S_{\alpha\alpha}$ is negative. But for any β, $-S_{\beta\beta} \leqslant -\min_\alpha S_{\alpha\alpha}$, where the function $\min_\alpha$ refers to the minimum of the three eigenvalues of the rate of strain tensor. Also $\overline{u_1 u_1} + \overline{u_2 u_2} + \overline{u_3 u_3} = 2k$. It follows that

$$\mathcal{P} \leqslant 2k \max_\alpha(-S_{\alpha\alpha}). \tag{5}$$
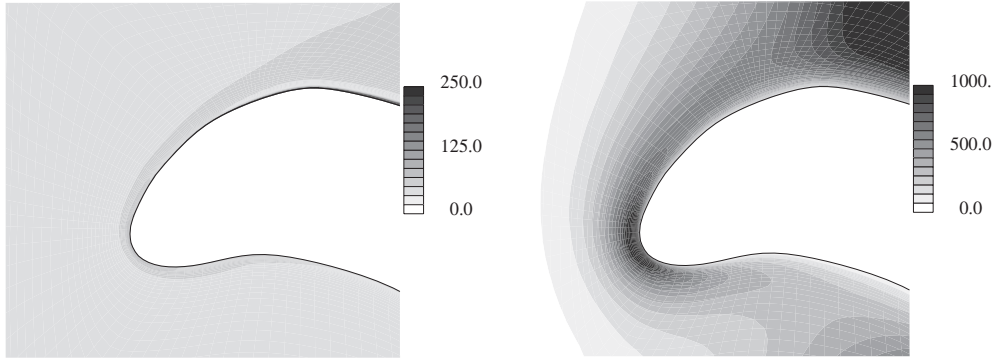
Figure 1. Contours of k with and without limiter. Scale is arbitrary, but the same in both views. The behavior to the right is anomalous.

It can be shown that

$$|S_{\alpha\alpha}| \leqslant \sqrt{2|\boldsymbol{S}|^2/3}$$

in three dimensions (Durbin 1996). This is derived by minimizing

$$|\boldsymbol{S}|^2 = S_{11}^2 + S_{22}^2 + (S_{11} + S_{22})^2.$$

(In two dimensions $|S_{\alpha\alpha}| = \sqrt{|\boldsymbol{S}|^2/2}$.) Hence, on purely mathematical grounds,

$$\mathcal{P} \leqslant 2k\sqrt{2|\boldsymbol{S}|^2/3}. \tag{6}$$

In particular, production should increase linearly with $|\boldsymbol{S}|$ at large rates of strain. However, with the eddy viscosity constitutive model

$$-\overline{u_i u_j} = 2\nu_T S_{ij} + \tfrac{2}{3}\delta_{ij}k, \tag{7}$$

equation (4) becomes

$$\mathcal{P} = 2\nu_t |\boldsymbol{S}|^2. \tag{8}$$

Production appears to increase quadratically with rate of strain.

Alternatively, inserting equation (8) into equation (6) gives the bound

$$\nu_t \leqslant \sqrt{\frac{2}{3}} \frac{k}{|\boldsymbol{S}|}. \tag{9}$$

Note the similarity of equations (3) and (9); both limit ν_T by a factor times $k/|\boldsymbol{S}|$. However, the former is more stringent, and is confined inside of the boundary layer by the blending function. Constraint (9) is needed outside boundary layers, in highly strained flow. Instead of phrasing (9) as a bound on eddy viscosity, it can be stated as the timescale bound

$$T \leqslant \frac{2}{\sqrt{6}C_\mu |\boldsymbol{S}|}.$$

This result, with a different numerical factor, can also be derived as a realizability condition (Durbin 1996). The Schwartz inequality requires that $0 \leqslant \text{e.v.}(\overline{u_i u_j}) \leqslant 2k$, or that the eigenvalues of the Reynolds stress be less than twice the turbulent kinetic energy, and be non-negative. That is a constraint on the constitutive model. The linear, eddy viscosity

formula (7) can be subjected to this condition. Analysis then leads to the stronger constraint

$$T \leqslant \frac{1}{\sqrt{6}C_\mu |\boldsymbol{S}|}. \tag{10}$$

It can be met in various ways; perhaps the simplest is via a limiter. For instance, condition (10) can be implemented for the k–ω model by

$$C_\mu T = \min\left[\frac{1}{\omega}, \frac{\alpha}{\sqrt{6}|\boldsymbol{S}|}\right]. \tag{11}$$

The form (2) with $T = 1/(C_\mu \omega)$ was assumed for ν_T. In equation (11), α is an adjustable constant. The bound (10) is satisfied for any $\alpha \leqslant 1$: in Medic and Durbin (2002), $\alpha = 0.6$ was selected for all models. The constraint is derived as a matter of principle, not restricted to a particular class of flow. Hence, it can come into effect in shear layers, where it usually is not needed. The constant of 0.6 was selected, in part, to make the constraint inoperative within shear layers.

Many investigators have proposed to make model constants functions of the rate of strain. Zhu and Shih (1993) invoke a strain-dependent formula for C_μ based on realizability of the constitutive formula (7) in two dimensions. Equation (9) can alternatively be phrased as

$$C_\mu \leqslant \sqrt{\frac{2}{3}} \frac{\varepsilon}{|\mathbf{S}|k}.$$

Rather than a limit *per se*, Zhu and Shih (1993) propose the formula

$$C_\mu = \frac{2/3}{5.5 + |\mathbf{S}|k/\varepsilon}$$

to effect a bound.

Realizability of the Reynolds stresses is not a compelling argument. The mean flow is computed from the eddy viscosity. The Reynolds stress tensor, *per se*, is not used. The real issue is to avoid excessive production of turbulent energy. Equation (6) is the essential bound. Even when implemented as a timescale bound, Sveningsson and Davidson (2004) show that the primary effect is on production of turbulent energy. Their paper contains recommendations on limiters for the v^2–f model. They recommend not applying the bound (10) to the timescale that appears in the source of the f-equation—that is, T in equations (28) and (29). An early method to constrain production of turbulent kinetic energy production is that of Launder and Kato (1993). They replaced the formula $\mathcal{P} = \nu_T |S|^2$ by $\mathcal{P} = \nu_T |S \parallel \Omega|$. This is not consistent with equation (6); rather it is designed to make production vanish in pure straining flow.

Figure 2, based on Seo (2004), shows how various limiters affect turbulent intensity on the stagnation line of a blunt body. The geometry is a flat strip, with a filled wake, designed to avoid separation (Bearman 1972) as is shown in the upper portion of this figure. The data were measured for various inlet turbulence levels and are normalized by the initial k. Figure 2(a) shows how k is produced excessively by the standard k–ε model: the same is seen with k–ω. The various methods in figure 2 of constraining production to grow no more rapidly than $|\boldsymbol{S}|$ at large rates of strain bring k closer to data, but the computed k/k_0 is still above the data in all cases. The limiters leave room for empiricism; benchmark data are needed to settle model constants. However, data on k are not ideal for that purpose. Eddy viscosity models are meant for mean flow prediction, so mean flow data should be the basis for calibration.

An example of the effect of timescale limiting on mean heat transfer is provided in figure 3, from Medic and Durbin (2002). This figure shows heat transfer to a blade in a
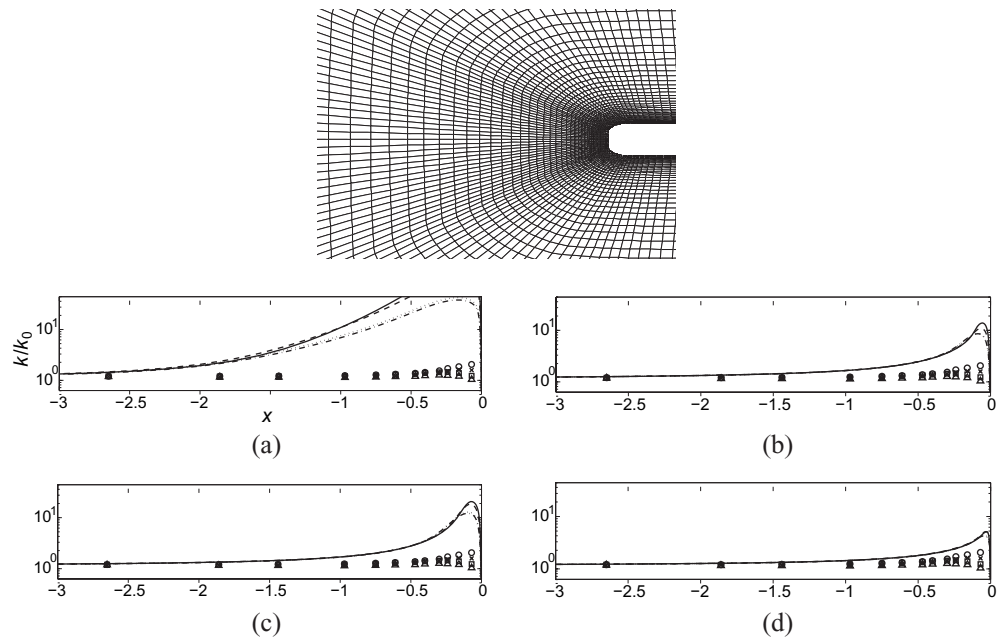
Figure 2. Kinetic energy on the stagnation line of a bluff body. (a) Baseline k–ε model; (b) k–ε with timescale limit; (c) k–ε with strain-dependent C_μ; (d) v^2–f with timescale limit. Symbols are data from Bearman (1972).
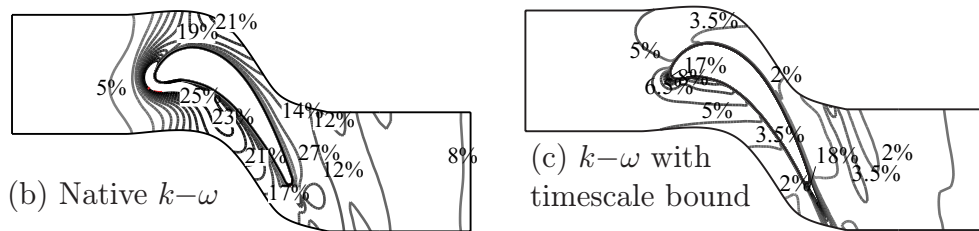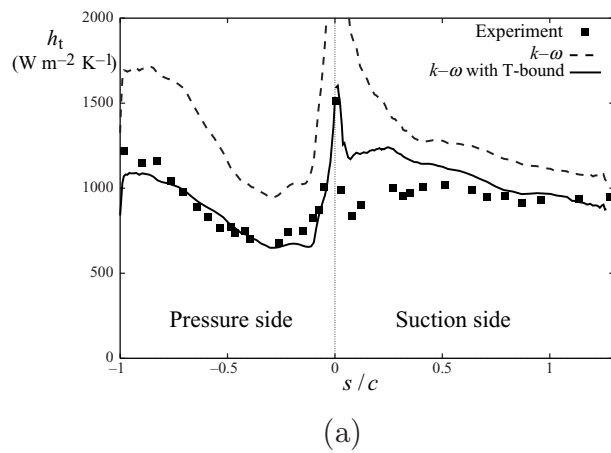
Figure 3. Heat transfer coefficient (a) and turbulent intensity $\sqrt{2k/3}/U$ in percentage (b and c). In (a), - - - is the native k–ω model and —— is k–ω with the bound (11).

linear turbine cascade. The development of turbulent intensity in the blade passage is shown by the lower panels. Turbulent intensity is defined locally as $\sqrt{k}/U(x)$. Both numerator and denominator increase in strongly accelerated flow, but it is known from experiment and theory that the ratio decreases. Without limiting the rate of energy production, the k–ω model predicts a substantial increase of the ratio; hence it is in error. When the timescale is bounded as in equation (11), a qualitatively correct behavior is obtained. The uppermost panel of figure 3 illustrates the effect on heat transfer. Excessive energy production leads to excessive heat transfer. With the timescale bound imposed, agreement with data is improved.

3. Wall functions revisited

The wall function is a time-honored, pragmatic device. Its virtues are to reduce the number of grid points in a computational analysis and to avoid the need to solve stiff, discretized equations in the near-wall region. At high Reynolds number, the viscous wall layer is extremely thin. A very fine mesh is needed to resolve it.

A wall function should not be understood as a separate formulation that is patched onto the turbulence model. The wall function and the solution to the turbulent transport model should merge seamlessly. In practice, the wall function is a boundary condition rather than an overlap law, but its concept is of an overlap. In that conception, the wall function represents the inner region and the turbulence model represents the outer region. They have a common region of validity. The switch from wall function to turbulence model can occur anywhere within that overlap region.

To accomplish the aim of smooth mitering, the wall function can be formulated as an equilibrium solution to the full transport model. Sufficiently close to the wall the equilibrium simplifications will be accurate. Near-wall equilibration provides a basis for a consistent formulation.

Although wall functions have a reputation for being a frequently inaccurate patch, in fact they are based on classical notions that underlie our understanding of turbulent boundary layers. In theory, two regions can be delimited in the turbulent boundary layer, the 'law of the wall' and the 'law of the wake'. The former is of universal character; the latter is geometry-dependent. The law of the wall applies in a thin layer next to the surface. Universality of the wall layer implies that variables scaled on '+' units will collapse, independently of geometry or pressure gradient.

Thus, the mean velocity, tangential to the surface, is written as

$$U = u_* F(y_+), \tag{12}$$

where $y_+ = y u_*/\nu$. Dependence on the particulars of the flow enter implicitly through the friction velocity, $u_* \equiv \sqrt{\tau_w/\rho}$, where τ_w is the surface shear stress.

The wall layer can be characterized as a turbulent Couette layer—that is, as a layer of constant stress: $\tau = \tau_w = \rho u_*^2$. If an eddy viscosity is invoked for the Reynolds shear stress, then the constant total stress is obtained from the sum of molecular and eddy viscosity:

$$-\overline{uv} + \nu \partial_y U = (\nu_T + \nu)\partial_y U.$$

The universal function in equation (12) is found by equating this to u_*^2:

$$U_+ = \int_0^{y_+} \frac{\mathrm{d}y_+}{1 + \nu_T^+}. \tag{13}$$

Given eddy viscosity distribution, $\nu_T^+(y_+)$, equation (13) provides the mean velocity.

From time to time, it has been proposed to treat the wall layer as a Couette–Poiseulle flow—that is, as a linear stress layer (Craft *et al* 2002; Knopp *et al* 2006; Popovac and Hanjalic 2007). For instance, if the right side of the thin-layer momentum equation

$$\frac{\partial \tau}{\partial y} = \frac{DU}{Dt} - \frac{\mathrm{d}P}{\mathrm{d}x}$$

is treated as a constant, C_a, then $\tau = \tau_w + C_a y$. With this, equation (13) becomes

$$U_+ = \int_0^{y_+} \frac{(1 + \alpha y_+)\mathrm{d}y_+}{1 + \nu_T^+}, \tag{14}$$

where α is a non-dimensional acceleration parameter. Stratford's half-power law is recovered when α is large and non-dimensional variables are rescaled on α (Townsend 1976). An aside: it can be shown that the k–ε model does not have a solution for the half-power law $U \sim (C_a y)^{1/2}$.

Commonly, wall functions are restricted to large y_+ within the law of the wall layer (and $\alpha = 0$). If $y_+ \gtrsim 40$, then further theoretical reasoning shows that the velocity assumes a logarithmic form

$$U_+ = \frac{1}{\kappa} \log(y_+) + B, \tag{15}$$

where $\kappa = 0.41$ is von Karman's constant, and the additive constant B is about 5.1. In practice, this is rearranged as a friction law

$$u_* = \kappa U(1)/[\log(y(1)u_*/\nu) + \kappa B] \tag{16}$$

in terms of computational data at the wall adjacent node, $y(1)$. In a finite-volume formulation, $\tau_w = \rho u_*^2$ provides the momentum flux on the wall face; in a finite difference approach, u_* determines the normal derivative of velocity, as in $\partial_y U = u_*/\kappa y(1)$.

To avoid ill-posedness as u_* changes sign, the boundary conditions on turbulence variables are usually expressed in terms of the velocity scale, $u_k \equiv (k\sqrt{C_\mu})^{1/2}$. They assume the form (Launder and Spalding 1974)

$$\frac{\partial U}{\partial y} = \frac{\tau_w}{\rho \kappa u_k y(1)}, \qquad \varepsilon = \frac{u_k^3}{\kappa y(1)}, \qquad \frac{\partial k}{\partial y} = 0. \tag{17}$$

But it is not necessary to apply the wall function in the log layer. Equation (16) can be cast generally as

$$u_* = U(1)/[F(y_+(1)]$$

for any point within the wall layer, via equation (12).

Various methods have been proposed to extend the validity of wall functions to $y_+ \lesssim 40$ in the interest of more flexible meshing. Perhaps the simplest proposal is the scalable wall function of Vieser *et al* (2002). They replace y_+ by $\max(y_+, 11)$ and apply a conventional wall function at this point. This constrains the lowest grid point to lie above the wall. It implies that the geometry is distorted such that the mesh lies above the viscous layer.

Other approaches accept that the mesh is defined by the true geometry and modify the wall function to accommodate low values of y_+. For instance, Launder and Spalding (1974) proposed the interpolation formula

$$y_+ = U_+ + \mathrm{e}^{-\kappa B}\left(\mathrm{e}^{\kappa U_+} - 1 - \kappa U_+ - \frac{1}{2}(\kappa U_+)^2 - \frac{1}{6}(\kappa U_+)^3\right) \tag{18}$$

valid from the wall to the top of the log layer. Equation (18) can be solved, in place of the log law, for u_*.

Conditions (17) for the turbulence variables might be extended to low y_+ as follows. Given that the near-wall region is a constant stress layer, the total non-dimensional stress is $(1 + \nu_{T_+})\partial_{y_+} U_+ = 1$. From this

$$\nu_{T+} = \partial y_+ / \partial U_+ - 1 = \kappa e^{-\kappa B} \left(e^{\kappa U_+} - 1 - \kappa U_+ - \frac{1}{2}(\kappa U_+)^2 \right), \qquad (19)$$

where $\nu_{T+} = \nu_T / \nu$. Formula (19) provides a boundary condition on $C_\mu k T = \nu_T$. For instance, if k is known, it gives the boundary value of $\omega = k/(\nu \nu_{T+})$ or of $\varepsilon = C_\mu k^2/(\nu \nu_{T+})$ in the k–ω and k–ε models. Commonly, the condition $\partial_y k = 0$ on k is retained—even though it is not valid below $y_+ = 40$. If the k found with this (incorrect) boundary condition on k is combined with equation (19) to provide a boundary condition on ω (or ε) in the viscous wall layer, they would ensure a suitable eddy viscosity, albeit both k and ε would differ from their observed near-wall behavior.

Formula (15) avoids the need to specify ν_T^+; however, it places a severe constraint on computational grids. In the wall function method, the first computational node is above the wall, say at $y_+(1)$. Between the wall and $y_+(1)$, the universal law of the wall is invoked. For the log law (15) to be obtained, the first grid point must be sufficiently far from the wall. In general, a grid will not meet this; indeed, the condition that the first node be far enough from the wall is a constraint that the near-wall mesh should be sufficiently coarse—for instance, if $y_+(1) = 40$ is a cell center, then $y_+(2) = 3y_+(1) = 120$. Such a coarse grid is contrary to the conditions for numerical accuracy.

The general notion of a wall function does not imply coarseness of the grid. The first grid point can lie at any $y_+(1)$ within the universal wall layer. It can be quite near the surface. Specifications of $F(y_+)$ that are valid at any y_+ in the wall layer have been available for several decades. They are in the form either of interpolations, such as 18, between the log law and the linear, viscous sublayer profile: $U_+ = y_+$, $y_+ \to 0$; or of a switch between log and linear profiles at $y_+ \approx 11$. However, turbulence variables have been treated in an inconsistent manner. For instance, the log-layer condition $\partial_y k = 0$ has been applied below the log layer, where it is erroneous.

The mean velocity is provided by equation (13). For the turbulence variables, Vieser *et al* (2002) and Popovac and Hanjalic (2007) propose interpolation functions between the viscous, v, and outer, o, regions of the wall layer. Vieser *et al* (2002) construct the universal function as

$$\phi = \sqrt{\phi_v^2 + \phi_o^2}.$$

Popovac and Hanjalic (2007) use

$$\phi = e^{-\Gamma}\phi_v + e^{-1/\Gamma}\phi_o, \qquad \Gamma = \frac{0.01 y_+^4}{1 + 5y_+},$$

where ϕ is the variable being interpolated. For the ε boundary condition,

$$\varepsilon_v = 2\nu k/y^2 \text{ and } \varepsilon_o = C_\mu^{3/4} k^{3/2}/\kappa y.$$

Knopp *et al* (2006) follow the same approach for interpolating the ω boundary condition. They use

$$\omega = \Gamma(\omega_v + \omega_o) + (1 - \Gamma)(\omega_v^{1.2} + \omega_o^{1.2})^{1/1.2}, \qquad \Gamma = \tanh[y_+^4/10^4]$$

9
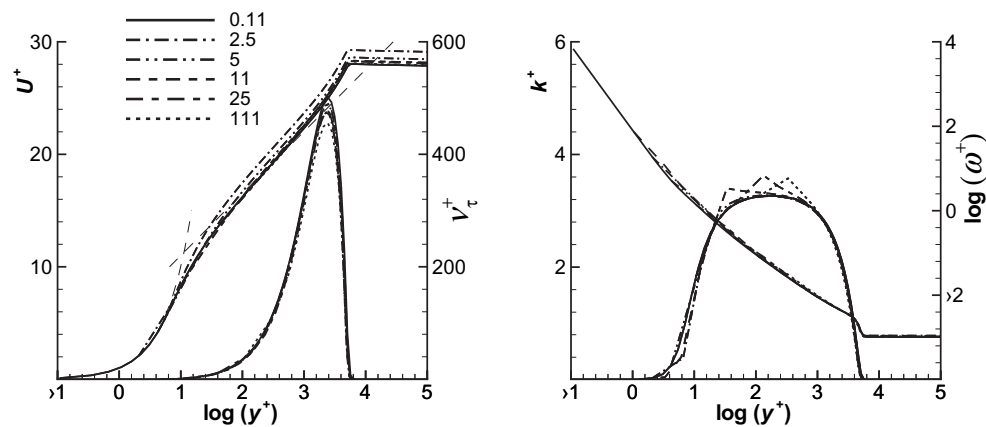
Figure 4. Velocity, eddy-viscosity profiles; profiles of k and ω in a flat plate boundary layer. Legend cites the y_+ matching point.

with

$$\omega_\mathrm{v} = 6\nu/\beta_\omega y^2 \quad \text{and} \quad \omega_\mathrm{o} = u_*/\sqrt{\beta_k}\kappa y.$$

The βs are model constants.

The interpolation function provides values at the first computational node next to the wall. If an interpolation function is invoked for ε or ω, equation (19) provides a condition for k that is consistent with the mean velocity interpolation. Again, as noted below (19), the resulting values of k and ε will not agree with data, but the eddy viscosity will be acceptable.

A properly formulated wall function should match smoothly all variables of the outer model. Then there is hope for grid insensitivity. Kalitzin *et al* (2005) advocate a method based on a look-up table. It is assumed that the turbulence model can be integrated with the wall on a fine grid, and the desire is to develop a technique to use coarse near-wall grids. It is also assumed that the Reynolds number is high enough for a law of the wall function (12) to be valid.

First, the turbulence model is solved on a fine grid in a boundary layer. Then the portion lying within the universal layer is saved to create a table that can be interpolated to provide a boundary value at $y_+(1)$. For instance, a solution to the k–ω model is normalized as

$$k = u_*^2 g(y_+), \qquad \omega = u_*^2/\nu\, h(y_+)$$

with g and h stored in tabular form. This approach provides consistency: a solution to the model is being used both above and below $y_+(1)$. One can hope that the match will be nearly seamless. Another way of looking at the notion that the formulation should be insensitive to the matching point is to view a properly posed wall function as providing an approximation to a full solution that would be obtained by accurately integrating with the wall.

That idea is tested in figure 4 for the k–ω model. The various curves are for the various $y_+(1)$ values indicated in the legend. The solid curve is an accurate integration with the wall. Ideally, the curves should lie atop one another. The curves are in close proximity. However, as $y_+(1)$ increases, the grid becomes coarser, and the discretization error increases. With that qualification, the wall function methodology appears to be successful. More elaborate testing (Kalitzin *et al* 2005) confirms the insensitivity to the matching point.
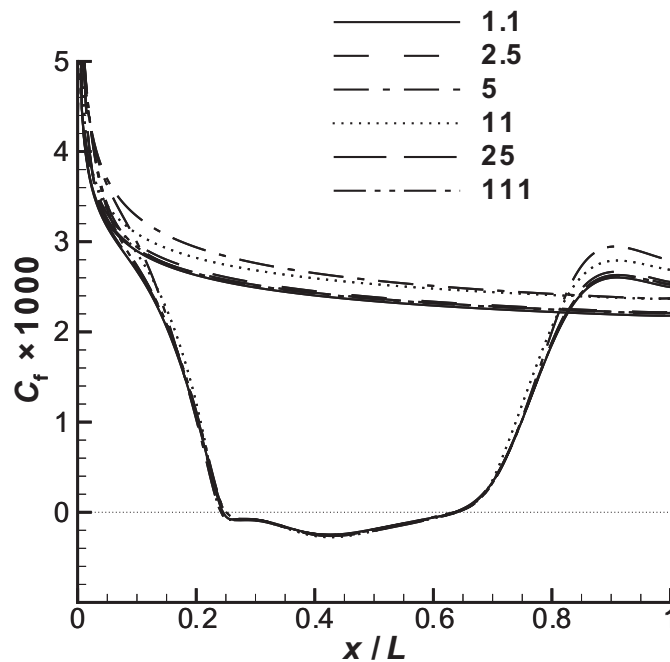
Figure 5. Skin friction: ZPG (upper) boundary layer and separation bubble (lower). The legend cites y_+ at the matching point.

Strong non-equilibrium violates the conditions for near-wall universality. In principle, wall functions are not justified for separated boundary layers. In practice, they can be used, and are. Figure 5 shows skin friction coefficients for two cases; the upper one is a flat plate and the lower one is a plate with pressure gradient-driven separation and reattachment. Curiously, the latter shows better insensitivity to the location of $y_+(1)$ than the former. In the recirculation region, $y_+ \equiv y u_*/\nu$ is reduced because u_* is small. That might be part of the reason for a better result; but the case with $y_+(1) = 111$ upstream still has $y_+(1) \approx 50$ in the separated region.

A method termed *analytical wall functions* is proposed in Craft *et al* (2002). Rather than specifying a condition for k in the wall adjacent cell, they solve its transport equation. They divide the wall adjacent cell into two layers: the viscous region and the log-law region. Formulae for $\mathcal{P}$ and ε are integrated over this cell to provide source terms in the k-equation. The mean flow is obtained from equation (14) where α is found from the momentum equation in the wall adjacent cell. The eddy viscosity is assumed to vanish below $y_*^v = 10.8$ and to increase linearly above that. Instead of standard + variables, these authors use $y_*^v \equiv \sqrt{k(1)}y/\nu$.

4. Surface roughness

Surface roughness can substantially affect transfer of momentum or heat between the fluid and wall. The viscous sublayer adjacent to a smooth wall presents a high impedance to transport to and from the surface; protrusions that penetrate the viscous layer increase transfer rates between the surface and the fluid. They do so by generating irregular, turbulent motion and by extending the surface into the flow.

Again, the emphasis of recent work has been on formulations of roughness effects that are useable on any mesh, irrespective of refinement, or coarseness, near the surface. The starting point is usually the log law for rough walls.

Intuitively, asperities on the surface will increase the drag force exerted by the wall on the flow. In a channel flow with a fixed pressure drop, the increased drag would decrease the mass flux and the centerline velocity. The additive constant, B, in equation (15) should decrease correspondingly. Let r be a scale for the size of the roughness. Assume that it is of the random, sandgrain, variety. The log law can be rewritten with y normalized by r and with r_+ defined as ru_*/ν:

$$U = u_* \left(\frac{1}{\kappa} \log[y/r] + \frac{1}{\kappa} \log(r_+) + B_r(r_+) \right)$$

$$= u_* \left(\frac{1}{\kappa} \log[y/r] + \mathcal{B} \right). \tag{20}$$

The function $B_r(r_+)$ represents the alteration of the additive constant by roughness.

The new additive term $\mathcal{B} \equiv \kappa^{-1} \log(r_+) + B_r(r_+)$ has been measured experimentally. Ligrani and Moffat (1986) fit the curve

$$\left. \begin{array}{ll} B_r = B, & r_+ < 2.25 \\ B_r = \xi(8.5 - \log(r_+)/\kappa - B) + B, & 2.25 \leqslant r_+ \leqslant 90 \\ B_r = 8.5 - \dfrac{1}{\kappa} \log(r_+), & r_+ > 90 \end{array} \right\} \tag{21}$$

through data for sandgrain roughness. This formula is broken into three regions: effectively smooth, transitionally rough and fully rough. The interpolation function ξ in the second line of (21) is

$$\xi = \sin\left(\frac{(\pi/2) \log[r_+/2.25]}{\log[90/2.25]} \right),$$

which increases from 0 to 1 through the transitionally rough range $2.25 \leqslant r_+ \leqslant 90$. The particular functional form for $B_r(r_+)$ depends on the nature of the roughness. The changes are primarily in the intermediate range of r_+ (Ligrani and Moffat 1986).

In the analytical wall function approach, $\nu_T = 0$ within the viscous wall layer $y < y_*^\nu$. Craft *et al* (2002) set $y_*^\nu = 10.8$ above smooth walls. Suga *et al* (2006) extended this to rough walls by moving the start of the viscous wall layer below 10.8 to

$$y_*^\nu = \max[10.8(1 - (h_*/70)^m), 0], \tag{22}$$

where h_* is the non-dimensional roughness height and

$$m = \max\left[(0.5 - 0.4(h_*/70)^{0.7}), (1 - 0.79(h_*/70)^{-0.28}) \right].$$

Variables with subscript * are normalized by $\sqrt{k}/\nu$: in the log layer, $y_+ = y_*/\sqrt{3.3}$.

Formula (22) causes the viscous sublayer to vanish over a fully rough wall, $h_* = 70$. However, Apsley (2007) found that y_+^ν must be allowed to go negative, and proposed the formula

$$y_+^\nu = \begin{cases} B - \dfrac{1}{\kappa} \log \kappa, & \text{if } B - \dfrac{1}{\kappa} \log \kappa > 0, \\ \dfrac{1}{\kappa}(1 - e^{\kappa(B - (\log \kappa)/\kappa)}), & \text{if } B - \dfrac{1}{\kappa} \log \kappa \leqslant 0. \end{cases} \tag{23}$$

This is in connection with a wall function method.
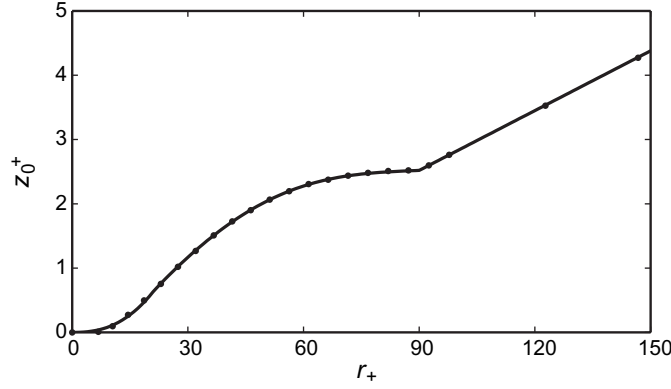
Figure 6. Calibration of the rough wall k–ω model (24).

Durbin *et al* (2001) and Seo (2004) propose a method that is applicable to models that are integrated to the wall, without wall functions. Consider the k–ω model. The boundary condition on a smooth wall is

$$k = 0, \qquad \omega = \frac{6\nu}{\beta y_1^2}.$$

When the wall is fully rough, the log layer is considered to extend to the surface, with no viscous sublayer (cf equations (22) and (21)). In the log layer, the solution to the k–ω model varies as

$$k = \frac{u_*^2}{\sqrt{C_\mu}}, \qquad \omega = \frac{u_*}{\kappa y \sqrt{C_\mu}}.$$

The k–ω wall roughness model interpolates between these. The following functions were used in the model of Seo (2004):

$$k = \frac{u_+^2}{\sqrt{C_\mu}} \min\left[1, \left(\frac{r_+}{90}\right)^2\right], \qquad \omega = \frac{6\nu}{\beta(y_1 + y_w)^2} \tag{24}$$

in which

$$y_w = \frac{\nu}{u_+} \left[\frac{6\kappa\sqrt{C_\mu}}{\beta} z_0^+\right]^{1/2}.$$

The eddy viscosity is now

$$\nu_T = k/\omega.$$

r_+ is the geometric roughness and z_0 is a *hydrodynamic roughness* length. The latter is regarded as a property of the model. It is calibrated so as to reproduce the log-layer displacement $\mathcal{B}$. Figure 6 shows the curve of z_0 versus r_+ that was obtained by reproducing the log-law displacement (21).

Wilcox (1993) proposed the simple roughness boundary condition

$$\omega = \frac{u_*^2}{\nu} S_r \tag{25}$$

13
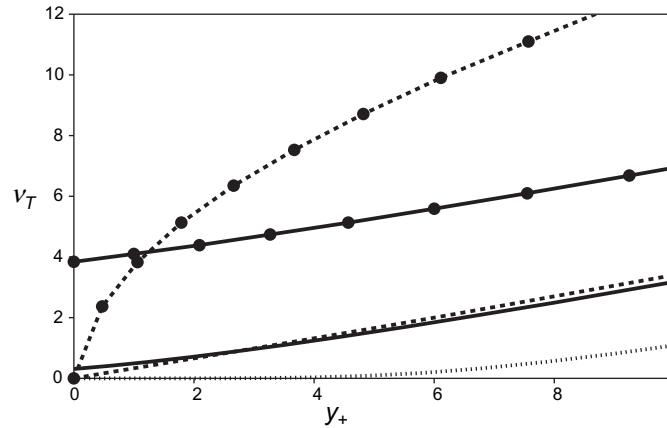
Figure 7. Eddy viscosity near a rough wall: — (Seo 2004); - - - (Wilcox 1993), $r_+ = 47$; •, $r_+ = 265$; ..., $r_+ = 0$.

with

$$S_r = \begin{cases} \left(\dfrac{50}{r_+}\right)^2, & 5 \leqslant r_+ \leqslant 25, \\[2mm] \dfrac{100}{r_+}, & r_+ > 25. \end{cases}$$

The boundary condition for k remains $k = 0$. Hence, the eddy viscosity k/ω vanishes, even at a rough wall. That is contrary to other models, such as formulae (22) and (23), for which the eddy viscosity is not zero under fully rough conditions. Figure 7 compares eddy viscosity profiles from Seo and Wilcox's rough wall k–ω models. For $r_+ = 47$, they differ only near the wall. However, for $r_+ = 265$ they differ considerably. Despite this large difference, Seo (2004) obtained very similar predictions for a number of test cases. Figure 8 contains velocity profiles at various locations along a ramp covered by sandpaper—a test case presented in Durbin *et al* (2001). The predictions of all models are virtually indistinguishable. In this experiment, the inlet roughness height is $r_+ = 360$, although it decreases to zero as the flow separates.

5. Elliptic relaxation method

The elliptic relaxation method was motivated by a desire to incorporate the suppression of mixing in consequence of wall blocking. The extent of the wall effect is determined by the turbulence length scale and by the wall geometry. The general form of the elliptic equation is

$$L^2 \nabla^2 f - f = -f_h, \tag{26}$$

where L is the turbulence scale and f_h is a source which depends on the particular type of model. The origin of equation (26) is discussed in Durbin and Pettersson-Reif (2001). It is shown there how correct near-wall behavior is obtained through this method, even when the homogeneous redistribution model, f_h, would be quite wrong. Proposals that modify the elliptic operator are discussed by Manceau *et al* (2001). They are motivated mostly by the behavior of f within the logarithmic layer. If f_h is a good model in the log layer, then

$x/d = 0.5$

$x/d = 0.71$

$x/d = 1.0$
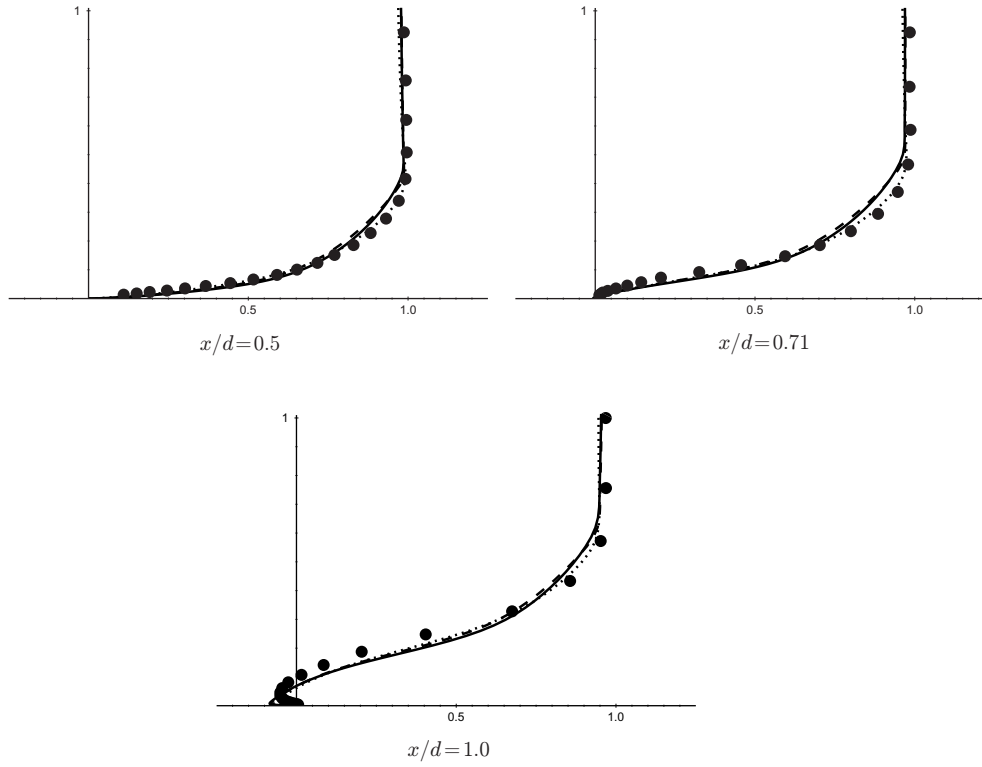
Figure 8. Velocity profiles in flow over a rough ramp. — (Seo 2004); - - - (Wilcox 1993); . . . (Durbin *et al* 2001); ●, experiment.

the elliptic term $L^2 \nabla^2 f$ should vanish there. Despite the modifications described in Manceau *et al* (2001), most applications of elliptic relaxation invoke the Helmholtz operator, as in equation (26).

Although elliptic relaxation can be applied to tensoral, Reynolds stress transport models, that would require f to be a tensor, with components f_{ij}. Recent applications have been restricted to scalar formulations. These include elliptic blending (Manceau 2005; Manceau and Hanjalic 2002), the $\zeta - f$ (Hanjalic *et al* 2005), $\phi - f$ (Laurence *et al* 2004) and $v^2 - f/k - \omega$ (Jones and Acharya 2005) models.

Elliptic blending invokes the f-equation

$$L^2 \nabla^2 f - f = -1. \tag{27}$$

Manceau and Hanjalic (2002) proposed to use f^2 as a blending function for Reynolds stress transport models. It functions as an interpolation of Reynolds stress source terms between the wall and the main flow. The boundary conditions are $f = 0$ at the wall and $f \to 1$ at infinity. For instance, the pressure strain is written as

$$\Pi_{ij} = f^2 \Pi_{ij}^h + (1 - f^2) \Pi_{ij}^w.$$

This is a source term in Reynolds stress transport equations. A unit vector $\hat{n} = \nabla f / |\nabla f|$ replaces the wall normal, which appears in earlier formulations of Π_{ij}^w. A full model can be found in Thielen *et al* (2004). Choi and Kim (2006) developed an elliptic blending model for heat transfer.

15

The same equation (27) was invoked with f playing the role of damping function for the k–ε model (Rahman and Siikonen 2007). Similar use of this equation has been made by others (Langer *et al* 2005). Note that a change of dependent variable to $\tilde{f} = f - 1$ will convert equation (27) to a homogeneous equation, with correspondingly altered boundary conditions. The equation is sometimes used in this alternative form.

However, in scalar models the f-equation is used differently from elliptic blending. The role of f is based on the physical notion that wall blocking is an elliptic effect. The wall *per se* enters via boundary conditions. The source term for the f-equation (26) is formed as an analogy to pressure–strain models: that is, it is a sum of slow and rapid parts:

$$f^h = \Pi_{\text{slow}} + \Pi_{\text{rapid}}.$$

The simplest form, based on the isotropization of production (IP) Reynolds stress closure model (Durbin and Pettersson-Reif 2001), is

$$\Pi_{\text{slow}} = C_1(2/3 - \zeta)/T, \qquad \Pi_{\text{rapid}} = C_2 P/k \qquad (28)$$

in which $\zeta = \overline{v^2}/k$. Hanjalic *et al* (2005) invoke the Speziale, Sarkhar and Gatski (SSG) model, and prescribe

$$\Pi_{\text{slow}} = (C_1 + C_2\mathcal{P}/\varepsilon)(2/3 - \zeta)/T, \qquad \Pi_{\text{rapid}} = 0 \qquad (29)$$

with $C_1 = 0.4$ and $C_2 = 0.65$.

If one accepts that second moment closures contain more physics than scalar models, then this provides a link to increased physics in the model. Alternatively, one can argue that $\overline{v^2}/k$ (or ζ) provides a measure of anisotropy. Near a boundary that anisotropy is critical to turbulent transport. Thus the eddy viscosity $\nu_T = C_\mu \overline{v^2} T$ is rewritten as $\nu_T = C_\mu \zeta k T$, where T is the turbulence timescale—$T = k/\varepsilon$ far from boundaries. In this sense, transport is suppressed by anisotropy ($\zeta < 2/3$); physically, the normal component of intensity is blocked by walls.

The f-equation was originally used as a source term in the $\overline{v^2}$ equation of the v^2–f model. Laurence *et al* (2004) and Hanjalic *et al* (2005) proposed that the dependent variable be changed to $\overline{v^2}/k$, denoting it as ϕ and ζ, respectively. Their transport equation is

$$\frac{D\zeta}{Dt} = f - \frac{\zeta}{k}\mathcal{P} + \nabla \cdot \left[\left(\nu + \frac{\nu_t}{\sigma_\zeta}\right)\nabla\zeta\right]. \qquad (30)$$

On a smooth wall $\overline{v^2} = 0 = \zeta = \phi$. Laurence *et al* (2004) invoke this same equation with the dependent variable renamed as ϕ and the additional source term

$$-\frac{2}{k}\frac{\nu_T}{\sigma_k}\nabla\phi \cdot \nabla k$$

on the right side. Their f-equation contains the negative of this on its left side. The motive for replacing $\overline{v^2}$ by ϕ or ζ is to make the boundary condition on f less stiff than in the v^2–f model. For the ϕ–f model, at walls $f = 0$; for the ζ–f model,

$$f \to -2\nu\zeta/y^2, \quad y \to 0.$$

These compare with the v^2–f condition

$$f \to -20\nu^2\overline{v^2}/\varepsilon y^4,$$

16

although the v^2–f model can be altered to make $f = 0$ the correct boundary condition (Wu and Durbin 2000). The $1/y^4$ coefficient causes numerical stiffness when $\overline{v^2}$ and f-equations are solved as a segregated pair; the stiffness is ameliorated by coupling them. The robustness of the ϕ–f and ζ–f models is demonstrated in Laurence *et al* (2004) and Hanjalic *et al* (2005).

The eddy viscosity is $v_T = C_\mu \overline{v^2} T = C_\mu \zeta k T$ with $C_\mu = 0.22$. The argument leading to formula (11) now implies

$$\tilde{T} = \min\left[\frac{k}{\varepsilon}, \frac{\alpha}{\sqrt{6} C_\mu \zeta |\mathbf{S}|}\right]. \tag{31}$$

Returning to the theme of section 2, a physical bound is imposed near walls. T is a correlation timescale. Although turbulent stresses vanish at a no-slip boundary, the correlation time does not. Theory and data show that it becomes proportional to the Kolmogoroff scale $(v/\varepsilon)^{1/2}$, which is finite at walls. Hence, equation (31) is further bounded as

$$T = \max[\tilde{T}, C_T (v/\varepsilon)^{1/2}],$$

where $C_T = 6$ is an empirical value.

These models are solved in conjunction with the standard k–ε transport equations. k and ε provide velocity, time and length scales that are needed in the f, $\overline{v^2}$, ϕ and ζ formulations. Jones and Acharya (2005) developed a version of the v^2–f model in which these scales are determined by the k–ω transport equations. They commented on the robustness of their model and demonstrated good predictions of the flow and surface heat transfer produced by film cooling jets.

Acknowledgments

References

Apsely D 2007 CFD calculation of turbulent flow with arbitrary wall roughness *Flow Turbulence Combust.* **78** 153–75

Bearman P W 1972 Some measurements of the distortion of turbulence approaching a two-dimensional bluff body *J. Fluid Mech.* **53** 451–67

Choi S-K and Kim S-O 2006 Computation of a turbulent natural convection in a rectangular cavity with the elliptic-blending second-moment closure *Int. Commun. Heat Mass Transfer* **33** 1217–24

Craft T J, Gerasimov A V, Iacovides H and Launder B E 2002 Progress in the generalized treatment of wall functions *Int. J. Heat Fluid Flow* **23** 148–60

Durbin P A 1996 On the k–ε stagnation point anomaly *Int. J. Heat Fluid Flow* **17** 89–90

Durbin P A 2004 Turbulence closure models for computational fluid dynamics *Encyclopedia of Computational Mechanics* vol 3 ed E Stein, R de Borst and T J R Hughes (New York: Wiley) pp 301–24

Durbin P A, Medic G, Seo J M, Eaton J E and Song S 2001 Rough wall modification of 2-layer k–ε *ASME J. Fluids Eng.* **123** 16–21

Durbin P A and Pettersson-Reif B A 2001 *Statistical Theory and Modeling for Turbulent Flows* (New York: Wiley)

Hanjalic K, Popovac M and Hadziabdic M 2005 A robust near-wall elliptic relaxation eddy-viscosity turbulence model for CFD *Int. J. Heat Fluid Flow* **25** 1047–51

Jones R and Acharya S 2005 Improved turbulence modeling of film cooling flow and heat transfer *Modelling and Simulation of Turbulent Heat Transfer* (Southampton, UK: WIT Press)

Kalitzin G, Medic G, Iaccarino G and Durbin P A 2005 Near-wall behavior of RANS turbulence models and implications for wall functions *J. Comput. Phys.* **204** 265–91

Launder B E and Kato M 1993 Modelling flow-induced oscillations in turbulent flow around a square cylinder *ASME Fluid. Eng. Conf.* **157** 189–99

Knopp T, Alrutz T and Schwamborn D 2006 A grid and flow adaptive wall-function method for RANS turbulence modelling *J. Comput. Phys.* **220** 19–40

Langer C A, Kassinos S C and Haire S L 2005 Application of a new algebraic structure-based model to rotating turbulent flows *Engineering Turbulence Modelling and Measurements 6* ed W Rodi and M Mulas (Amsterdam: Elsevier)

Launder B E and Spalding B 1974 The numerical computation of turbulent flows *Comput. Methods Appl. Mech. Eng.* **3** 269–89

Laurence D R, Uribe J C and Utyuzhnikov S V 2004 A robust formulation of the $v^2 - f$ model *Flow, Turbulence Combust.* **73** 169–85

Ligrani P M and Moffat R J 1986 Structure of transitionally rough and fully rough turbulent boundary layers *J. Fluid Mech.* **162** 69–98

Manceau R 2005 An improved version of the Elliptic Blending Model. Application to non-rotating and rotating channel flows *Proc. 4th Int. Synp. on Turbulence and Shear Flow Phenomena* (Williamsburg: VA)

Manceau R and Hanjalic K 2002 Elliptic blending model: a new nearwall Reynolds stress turbulence closure *Phys. Fluids* **14** 744–54

Manceau R, Wang M and Laurence D 2001 Inhomogeneity and anisotropy effects on the redistribution term in Reynolds-averaged Navier–Stokes modelling *J. Fluid Mech.* **438** 307–38

Medic G and Durbin P A 2002 Toward improved prediction of heat transfer on turbine blades *J. Turbomach.* **124** 187–92

Menter F R 1992 Two-equation eddy-viscosity turbulence models for engineering applications *AIAA J.* **32** 1598–605

Popovac M and Hanjalic K 2007 Compound wall treatment for RANS computation of complex turbulent flows and heat transfer *Flow Turbulence Combust.* **78** 177–202

Rahman M M and Siikonen T 2007 A simplified $v^2 - f$ model for near-wall turbulence *Int. J. Numer. Methods Fluids* **54** 1387–1406

Seo J-M 2004 Closure modeling and numerical simulation for turbulent flows: wall roughness model, realizability and turbine blade heat transfer *PhD Thesis* Stanford University

Suga K, Craft T J and Iacovides H 2006 An analytical wall-function for turbulent flows and heat transfer over rough walls *Int. J. Heat Fluid Flow* **27** 852–66

Sveningsson A and Davidson L 2004 Assessment of realizability constraints in $v^2 - f$ turbulence models *Int. J. Heat Fluid Flow* **25** 785–94

Thielen L, Hanjalic K, Jonker H and Manceau R 2004 Predictions of flow and heat transfer in multiple impinging jets with an elliptic blending second moment closure *Int. J. Heat Mass Transfer* **48** 1583–98

Townsend A A 1976 *The Structure of Turbulent Shear Flow* (Cambridge: Cambridge University Press)

Vieser W, Esch T and Menter F R 2002 Heat transfer predictions using advanced two-equation turbulence models *Technical Memorandum* CFX-VAL10/0602

Wilcox D C 1993 *Turbulence Modeling for CFD* (La Canada, CA: DCW)

Wu X and Durbin P A 2000 Boundary layer transition induced by periodically passing wakes *J. Turbomach.* **122** 442–9

Zhu J and Shih T-H 1993 Calculations of turbulent separated flows *NASA-TM* 106721